CHAPTER 3

Space Vector pulse width modulation

3.1 Introduction

The space-vector PWM technique is used to produce the switching control signals to be applied to the three-phase inverter. The SVPWM inverter is used to offer 15% increase in the dc link voltage utilization and low output harmonic distortions compared with the conventional sinusoidal PWM inverter. The control strategy of the SVPWM inverter is the voltage/frequency control method which is based on the space-vector modulation technique. For constant torque output, the air gap flux in the motor is maintained constant by operating on a constant voltage/frequency supply. However, the analysis assumes negligible winding resistance, where, in practical, at low frequencies the resistive voltage drop becomes significant compared with the induced voltage. This voltage drop causes a reduction in the air gap flux and motor torque. In order to maintain the low-speed torque, the voltage/frequency control method is used for controlling the speed of PMSM with performance accuracy.

3.2 Analysis and modeling of space-vector pulse width modulation technique

A three-phase two-level inverter shown in fig.1 provides eight possible switching states, made up of six active and two zero switching states. Active vectors divide plane for six sectors, where a reference vector *Vref* in fig.2 is obtained by switching on (for proper time) two adjacent vectors. It can be seen that vector *Vref* is possible to implement by the different switching on/off sequence of *V1* and *V2*.

The fundamental difference between SVPWM and SPWM is the existence of two additional zero voltage states V_0 (000), and V_7 (111). In addition to the six possible voltage vectors associated with the VSI, there are two zero voltage states associated with having all three of the positive pole switches on or all three of the negative pole switches on. This fact allows more output voltage since the third harmonic component exists. Thus, SVPWM is often considered as an eight state operation. Locus comparison of maximum linear control voltage in sine PWM and SVPWM is shown in fig. 3. The SVPWM generates less harmonics distortion in the output voltages or currents in comparison with SPWM, also the voltage utilization achieved by SVPWM is $2/\sqrt{3}$ times of SPWM.

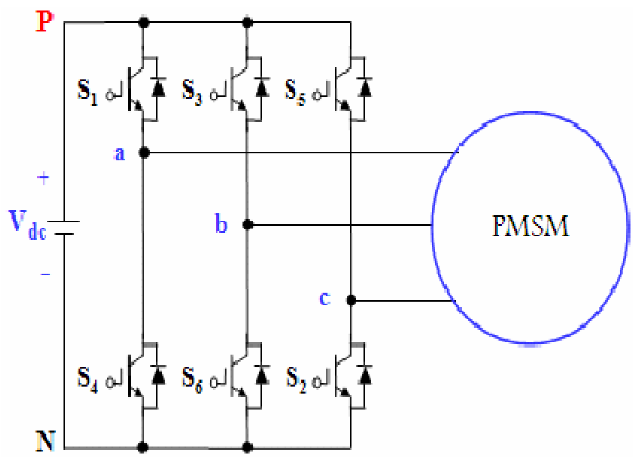

Fig. 3.1 Conventional three-phase voltage-source inverter bridge circuit

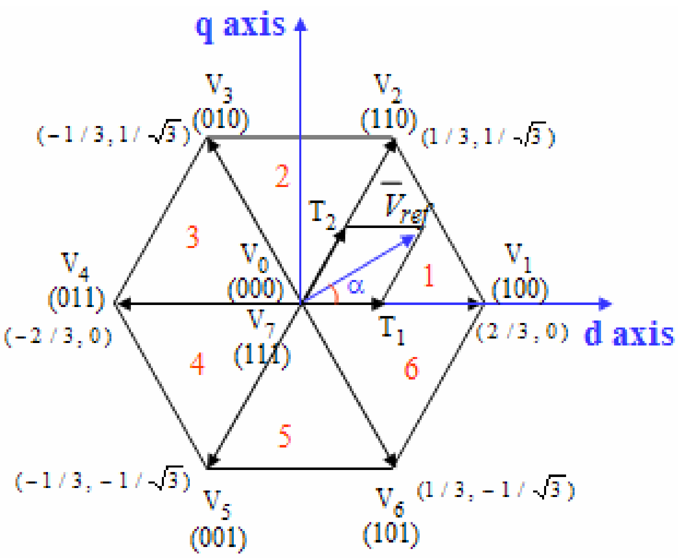

Fig. 3.2 the eight vectors in the stationary frame

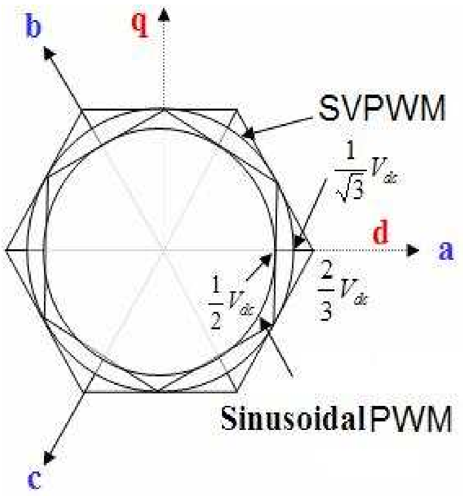

Fig. 3.3 Locus comparison of maximum linear control voltage in Sinusoidal PWM and SVPWM

To realize the SVPWM [1-5], first determine V_d, V_q, and angle α, secondly determine the time duration T_1, T_2, and T_0, thirdly determine the switching time of each switch **(S1 to S6).**

Step1: determination of the sector at which the vector is placed, this achieved by determination of the V_d, V_q, and angle α, According to the coordinate transformation in fig. 4

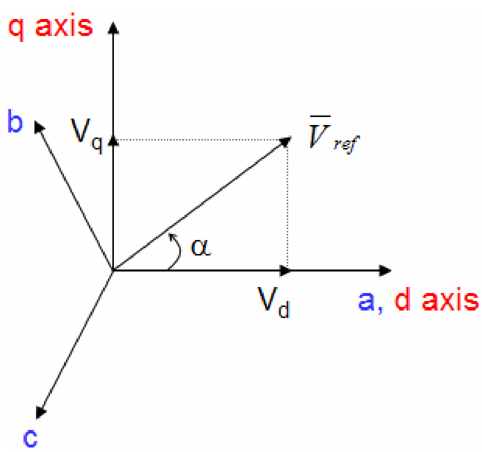

Fig. 3.4 Voltage Space Vector and its components in (d, q) coordinate

$$
\begin{aligned}
V_d &= V_{an} - V_{bn} \cdot \cos 60 - V_{cn} \cdot \cos 60 \\
&= V_{an} - \frac{1}{2} V_{bn} - \frac{1}{2} V_{cn}
\end{aligned}
$$

$$V_q = 0 + V_{bn} \cdot \cos30 - V_{cn} \cdot \cos30$$
$$= V_{an} + \frac{\sqrt{3}}{2} V_{bn} - \frac{\sqrt{3}}{2} V_{cn}$$

$$\therefore \begin{bmatrix} V_d \\ V_q \end{bmatrix} = \frac{2}{3} \begin{bmatrix} 1 & -\frac{1}{2} & -\frac{1}{2} \\ 0 & \frac{\sqrt{3}}{2} & -\frac{\sqrt{3}}{2} \end{bmatrix} \begin{bmatrix} V_{an} \\ V_{bn} \\ V_{cn} \end{bmatrix}$$

$$\left| \overline{V}_{ref} \right| = \sqrt{V_d{}^2 + V_q{}^2}$$

$$\alpha = \tan^{-1}\left(\frac{V_q}{V_d}\right) = \omega_s t = 2\pi f_s t$$

$$(\text{where, } f_s = \frac{1}{Ts})$$

According to the value of α we can find the sector number, such as $0 \le \alpha \le \frac{\pi}{3}$, gives sector 1.

Step 2: is to determine the time duration T_1, T_2, and T_0, and this is shown as in fig. 5, the reference vector expressed by a combination of two adjacent vectors, and the switching time duration at Sector 1 can be expressed as:

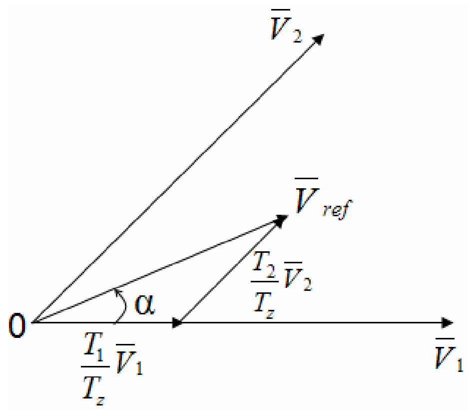

Fig. 3.5 Reference vector as a combination of adjacent vectors at sector 1

$$\int_0^{T_s} \overline{V}_{ref} = \int_0^{T_1} \overline{V}_1 dt + \int_{T1}^{T_1+T_2} \overline{V}_2 dt + \int_{T_1+T_2}^{Ts} \overline{V}_0$$

$$\therefore T_s \cdot \overline{V}_{ref} = (T_1 \cdot \overline{V}_1 + T_2 \cdot \overline{V}_2)$$

$$\Rightarrow T_s \cdot \left|\overline{V}_{ref}\right| \cdot \begin{bmatrix} \cos(\alpha) \\ \sin(\alpha) \end{bmatrix} = T_1 \cdot \frac{2}{3} \cdot V_{dc} \cdot \begin{bmatrix} 1 \\ 0 \end{bmatrix} + T_2 \cdot \frac{2}{3} \cdot V_{dc} \cdot \begin{bmatrix} \cos(\pi/3) \\ \sin(\pi/3) \end{bmatrix}$$

(where, $0 \le \alpha \le 60°$)

$$T_1 = T_s \cdot \frac{\left|\overline{V}_{ref}\right|}{\frac{2}{3} V_{dc}} \cdot \frac{\sin(\pi/3 - \alpha)}{\sin(\pi/3)}$$

$$T_1 = T_s \cdot \frac{\left|\overline{V}_{ref}\right|}{\frac{2}{3} V_{dc}} \cdot \frac{\sin(\pi/3 - \alpha)}{\frac{\sqrt{3}}{2}}$$

$$T_1 = T_s \cdot \frac{\left|\overline{V}_{ref}\right|}{\frac{1}{2} V_{dc}} \cdot \frac{\sin(\pi/3 - \alpha)}{\frac{2}{\sqrt{3}}}$$

$$\therefore T_1 = T_s \cdot m \cdot \frac{\sqrt{3}}{2}.\sin(\pi/3 - \alpha)$$

$$T_2 = T_s \cdot \frac{\left|\overline{V}_{ref}\right|}{\frac{2}{3} V_{dc}} \cdot \frac{\sin(\alpha)}{\sin(\pi/3)}$$

$$T_2 = T_s \cdot \frac{\left|\overline{V}_{ref}\right|}{\frac{2}{3} V_{dc}} \cdot \frac{\sin(\alpha)}{\frac{\sqrt{3}}{2}}$$

$$T_2 = T_s \cdot \frac{\left|\overline{V}_{ref}\right|}{\frac{1}{2} V_{dc}} \cdot \frac{\sin(\alpha)}{\frac{2}{\sqrt{3}}}$$

$$\therefore T_2 = T_s \cdot m \cdot \frac{\sqrt{3}}{2}.\sin(\alpha)$$

$$\therefore T_0 = T_s - (T_1 + T_2)$$

Switching time duration at any Sector

$$\therefore T_m = T_s \cdot m \cdot \frac{\sqrt{3}}{2} . \left(\sin\left(\frac{\pi}{3} - \alpha + \frac{n-1}{3}\pi \right) \right)$$

$$\therefore T_m = T_s \cdot m \cdot \frac{\sqrt{3}}{2} . \left(\sin \frac{n}{3}\pi - \alpha \right)$$

$$\therefore T_{m+1} = T_s \cdot m \cdot \frac{\sqrt{3}}{2} . \left(\sin\left(\alpha - \frac{n-1}{3}\pi \right) \right)$$

$$\therefore T_0 = T_s - T_1 - T_2, \quad \begin{pmatrix} \text{where, n} = 1 \text{ through } 6 \text{ (that is, Sector1 to 6)} \\ 0 \le \alpha \le 60° \end{pmatrix}$$

Step3: is used to determine the switching time of each switch by determine the modulating functions which compared with a triangle wave to give the predetermined patterns for the upper three switches, this is achieved by the table 1

Sector	Upper Switches (S_1, S_3, S_5)	Lower Switches (S_4, S_6, S_2)
1	$S_1 = T_1 + T_2 + T_0/2$ $S_3 = T_2 + T_0/2$ $S_5 = T_0/2$	$S_4 = T_0/2$ $S_6 = T_1 + T_0/2$ $S_2 = T_1+T_2+T_0/2$
2	$S_1 = T_1 + T_0/2$ $S_3 = T_1 + T_2 + T_0/2$ $S_5 = T_0/2$	$S_4 = T_2 + T_0/2$ $S_6 = T_0/2$ $S_2 = T_1+T_2+T_0/2$
3	$S_1 = T_0/2$ $S_3 = T_1 + T_2 + T_0/2$ $S_5 = T_2 + T_0/2$	$S_4 = T_1+T_2+T_0/2$ $S_6 = T_0/2$ $S_2 = T_1 + T_0/2$
4	$S_1 = T_0/2$ $S_3 = T_1 + T_0/2$ $S_5 = T_1 + T_2 + T_0/2$	$S_4 = T_1+T_2+T_0/2$ $S_6 = T_2 + T_0/2$ $S_2 = T_0/2$
5	$S_1 = T_2 + T_0/2$ $S_3 = T_0/2$ $S_5 = T_1 + T_2 + T_0/2$	$S_4 = T_1 + T_0/2$ $S_6 = T_1+T_2+T_0/2$ $S_2 = T_0/2$
6	$S_1 = T_1 + T_2 + T_0/2$ $S_3 = T_0/2$ $S_5 = T_1 + T_0/2$	$S_4 = T_0/2$ $S_6 = T_1+T_2+T_0/2$ $S_2 = T_2 + T_0/2$

Table 1 Switching Time Table at Each Sector

Limiting the hexagon

If the desired signal is outside the reachable space of the switching plane then the times $T_m + T_{m+1}$ is longer than T_s , it means the voltage saturation of the inverter. At this time, an over modulation should be performed to produce the maximum available voltage keeping its output with in hexagon limit. In this case the conduction times of the voltage vectors are represented as follows,

$$\therefore T'_m = \frac{T_s}{T_{m+1} + T_m} . T_m$$

$$\therefore T'_{m+1} = \frac{T_s}{T_{m+1} + T_m} . T_{m+1}$$

$$\therefore T_0 = 0$$

The physical effect of this algorithm is to reduce the magnitude of the output voltage, as long as the reference is inside the hexagon the output is unchanged and linearity is maintained. If the reference exceeds the limits of the hexagon, then the output is reduced to reset on the limit.

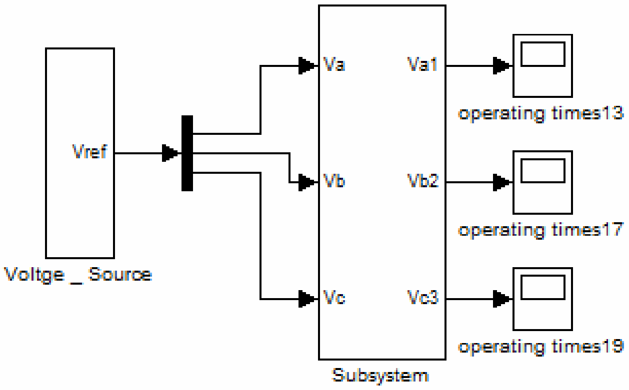

Fig. 3.6 Matlab Simulink model for SVPWM

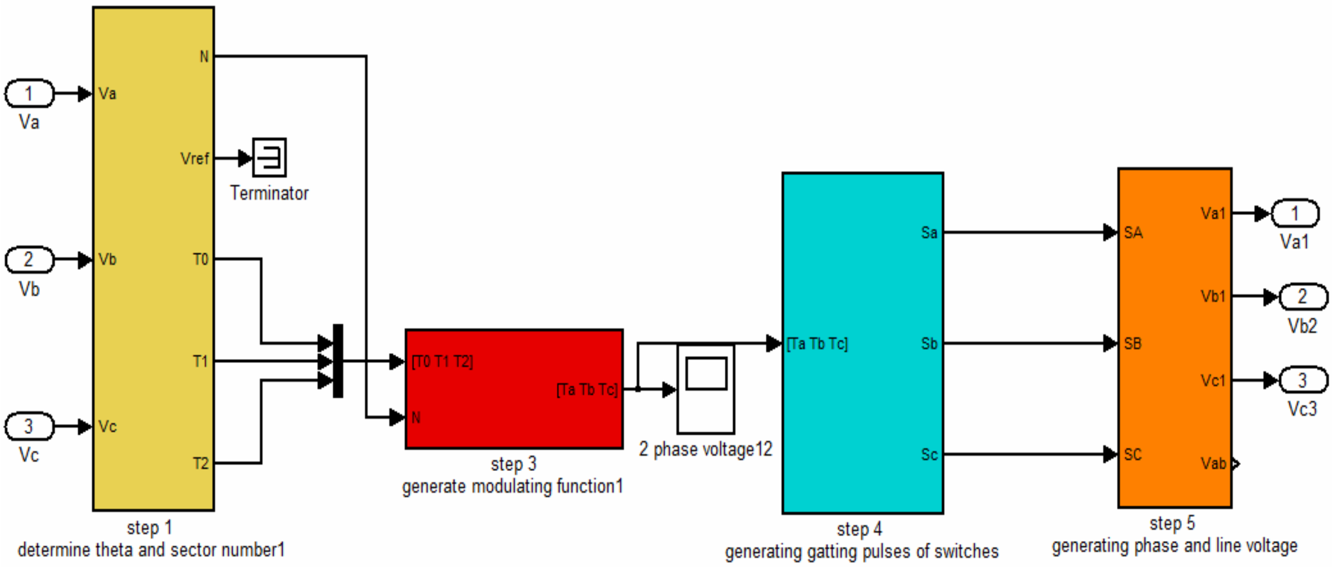

Fig. 3.7 Matlab Simulink under mask model for SVPWM indicating main steps

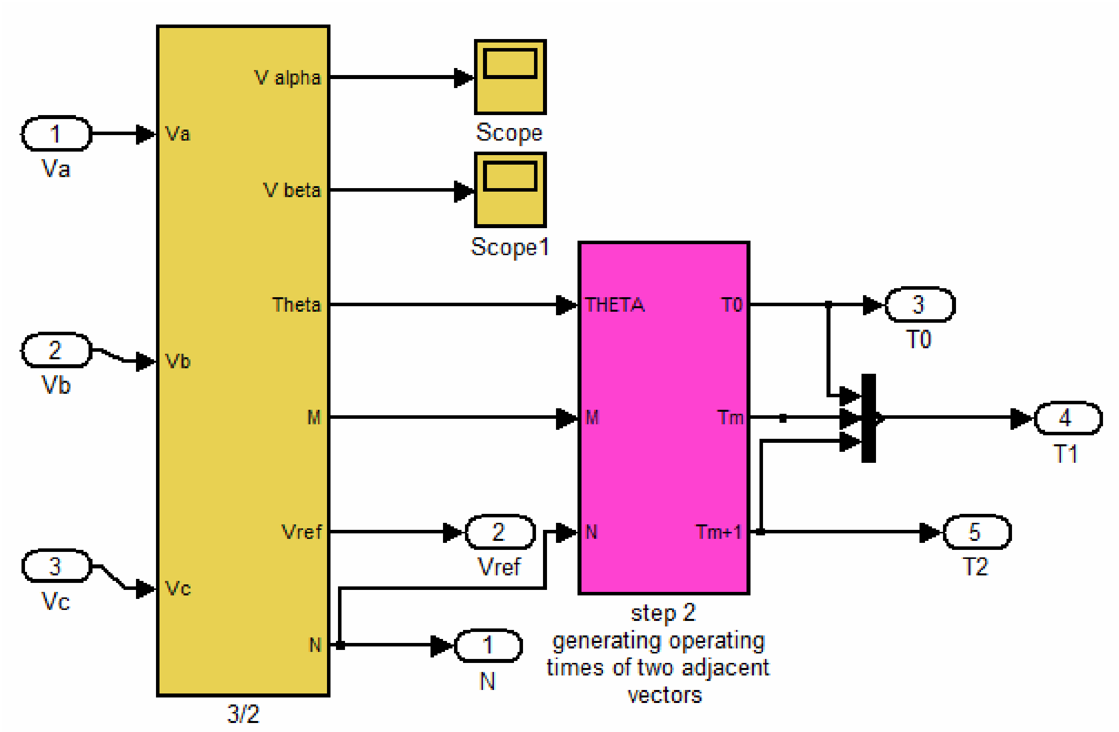

Fig. 3.8 Matlab Simulink under mask model for SVPWM indicating main steps

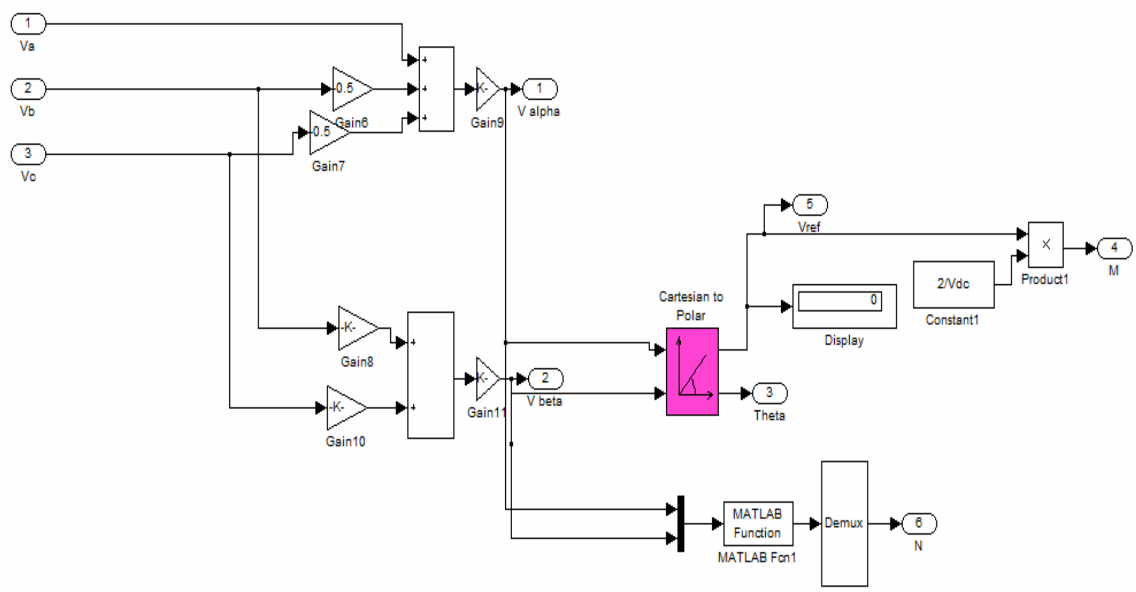

Fig. 3.9 Matlab Simulink under mask model for sector number determination, and modulation index determination

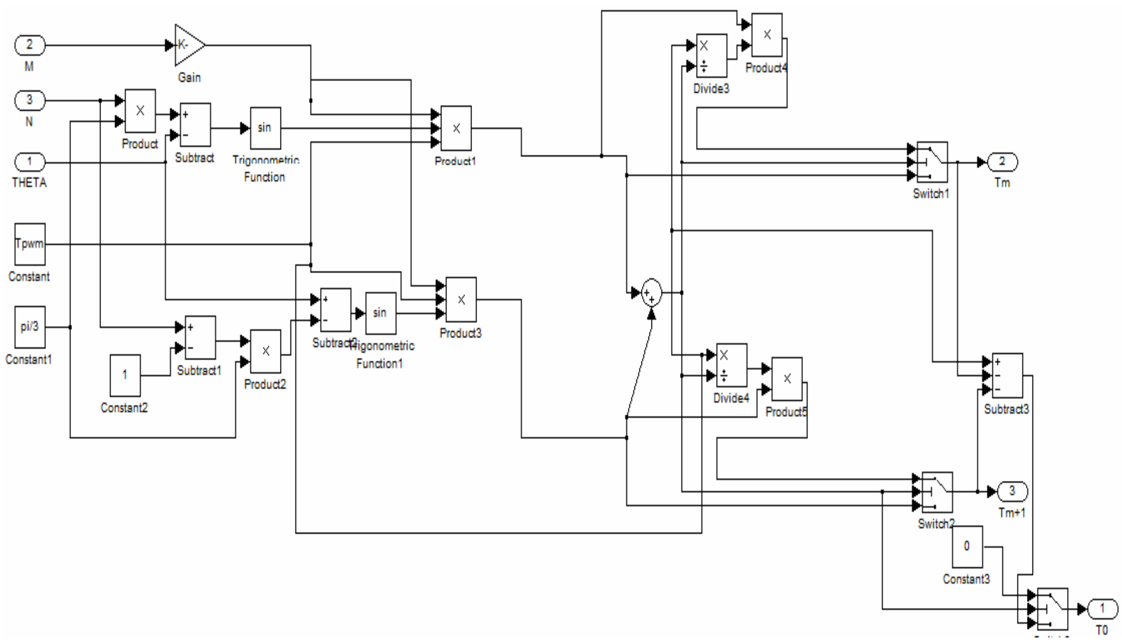

Fig. 3.10 Matlab Simulink under mask model for stitching times determination

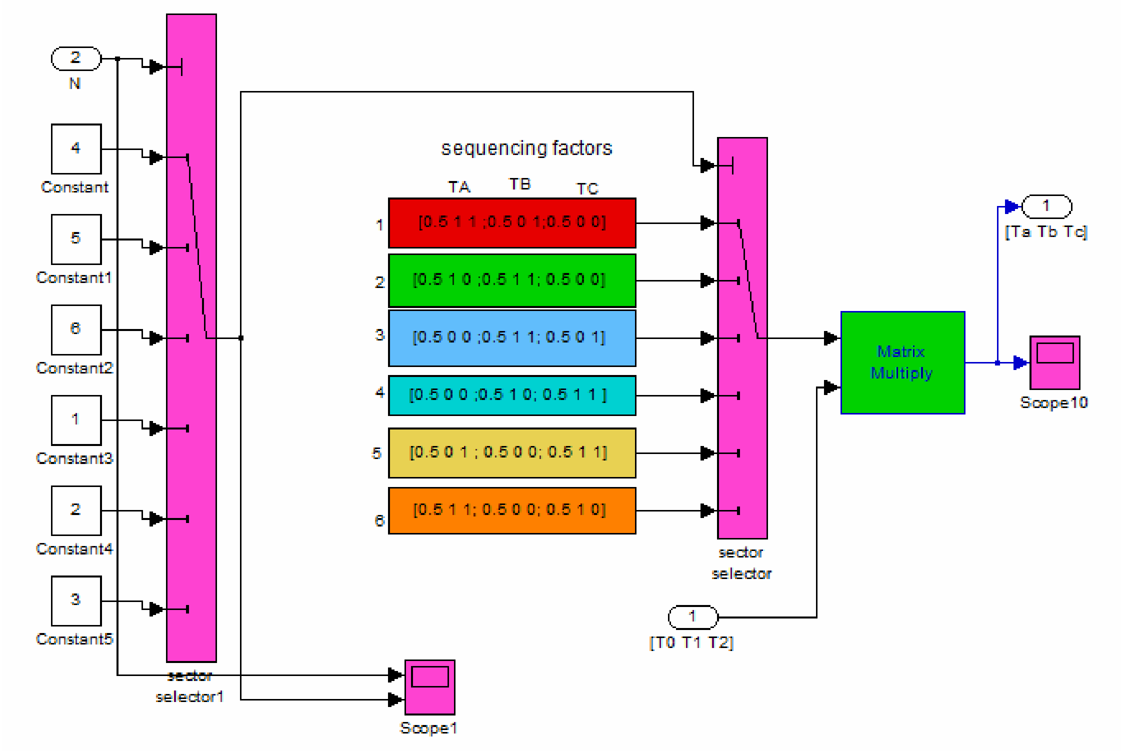

Fig. 3.11 Matlab Simulink under mask model for modulating functions determination

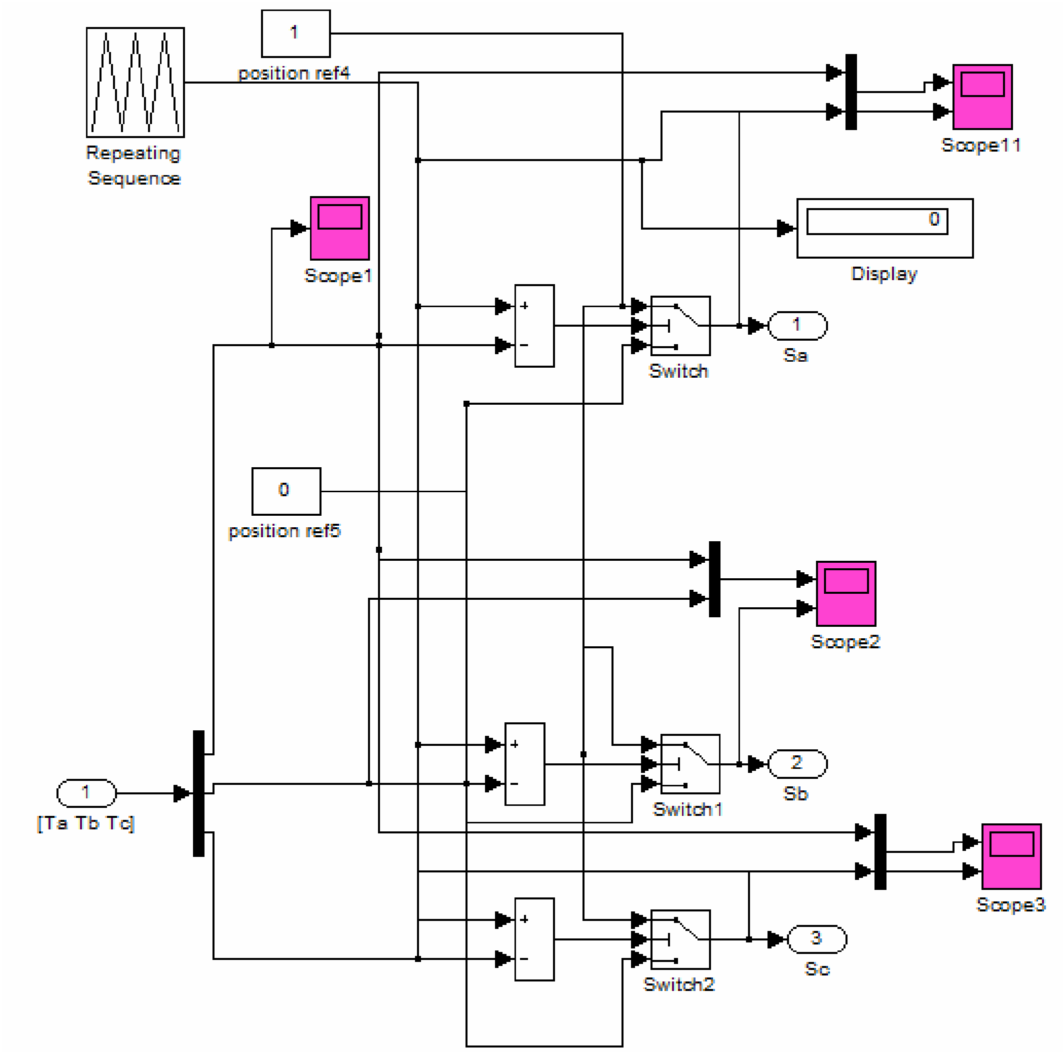

Fig. 3.12 Matlab Simulink under mask model for switching patterns determination

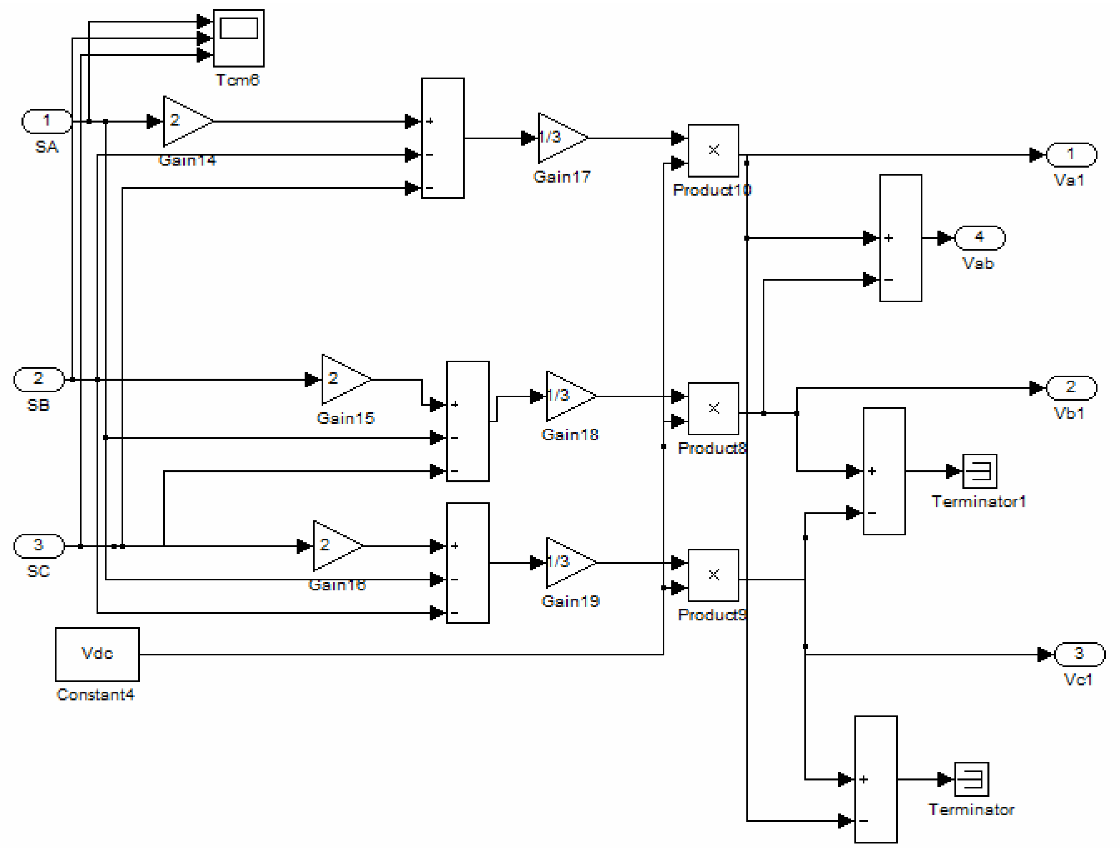

Fig. 3.13 Matlab Simulink under mask model for three- phase inverter

3.3 Simulation results

The simulation of the SVPWM-PMSM set is performed for 10 KHz and 5 KHz at fundamental frequency of 150 and 50 Hz for 0.95 Kw PMSM.

1-a 10 KHz switching frequency, 150Hz fundamental frequency, Vdc=570V, rated voltage= 230Vrms (325V peak), and modulation index m=1.1404

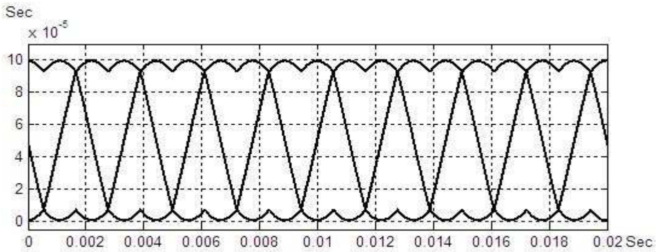

Fig. 3.14 Space vector modulating function a, b, c

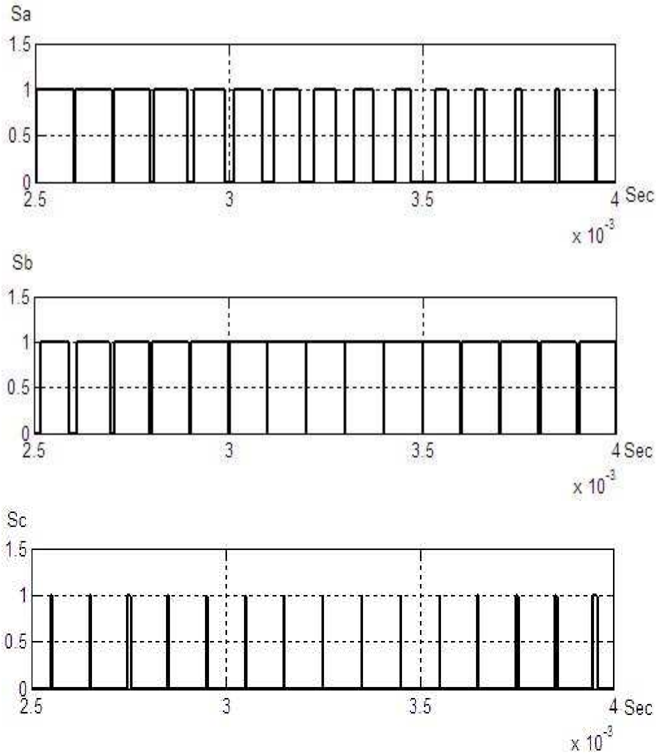

Fig. 3.15 Control signals for three upper switches of the inverter

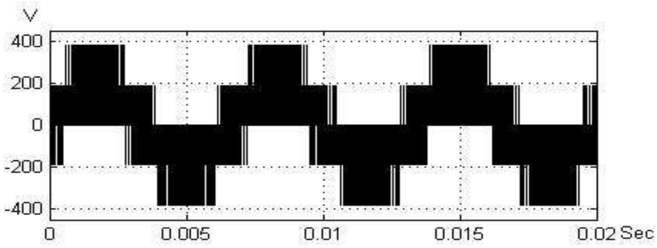

Fig. 3.16 Phase voltage of the motor Va

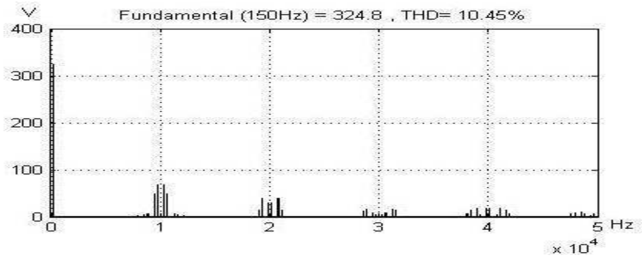

Fig. 3.17 Spectrum of phase voltage Va (peak value), and THD

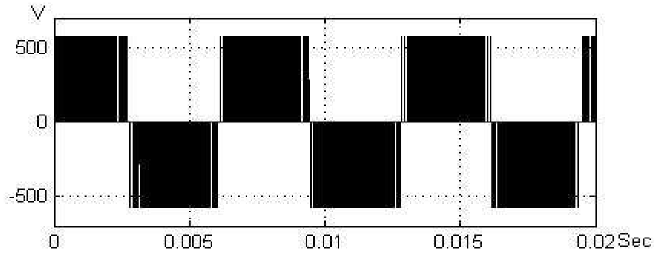

Fig. 3.18 Line voltage of the motor Vab

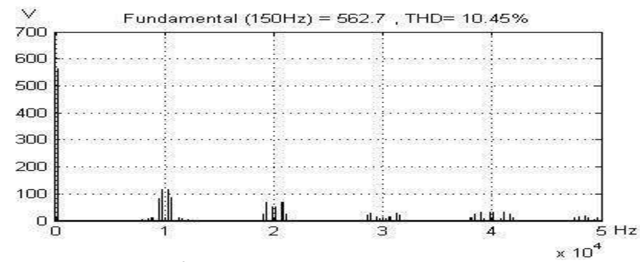

Fig. 3.19 Spectrum of Line voltage Vab (peak value), and THD

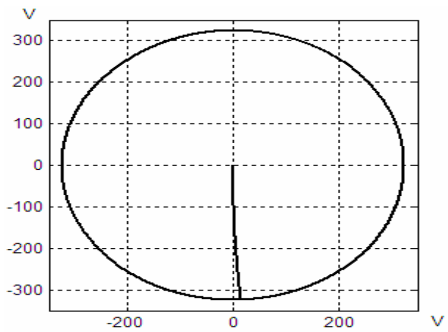

Fig. 3.20 Reference input voltage vector ($\alpha - \beta$)

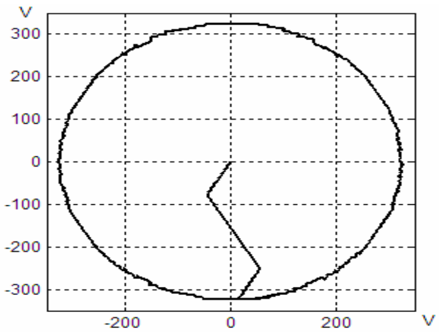

Fig. 3.21 Actual output voltage vector ($\alpha - \beta$)

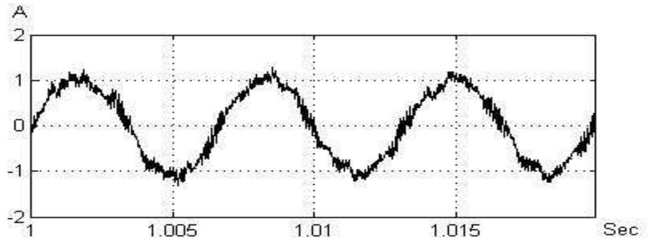

Fig. 3.22 Motor line current (Peak value) at half load Tl = 1.5 N.m

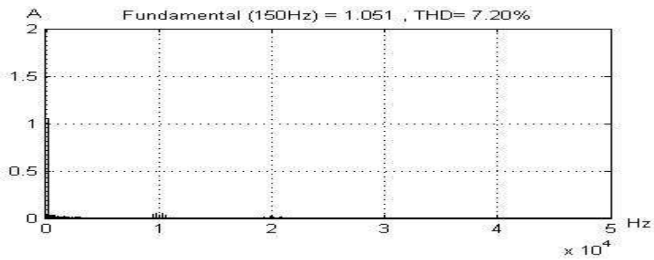

Fig. 3.23 Spectrum of motor line current (Peak value), and THD at half load Tl = 1.5 N.m

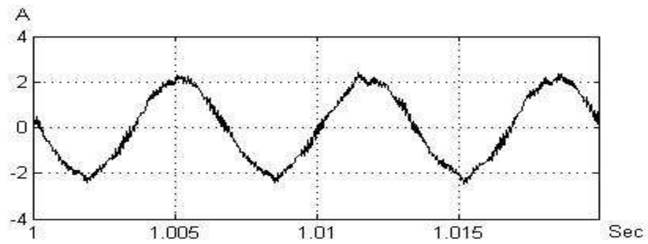

Fig. 3.24 Motor line current (Peak value) at full load Tl = 3 N.m

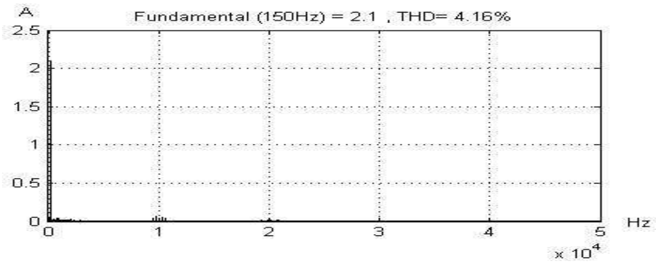

Fig. 3.25 Spectrum of motor line current (Peak value), and THD at full load Tl = 3 N.m

1-b 10 KHz switching frequency, 50Hz fundamental frequency, Vdc=570V, rated voltage= 76.667 Vrms (108V peak), and modulation index m=0.38

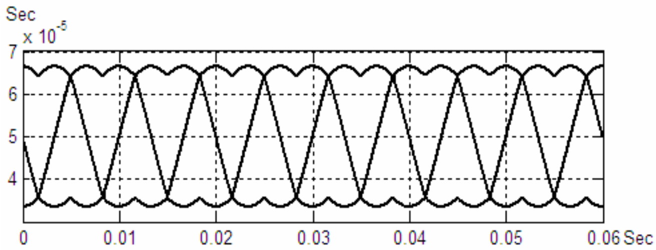

Fig. 3.26 Space vector modulating function a, b, c

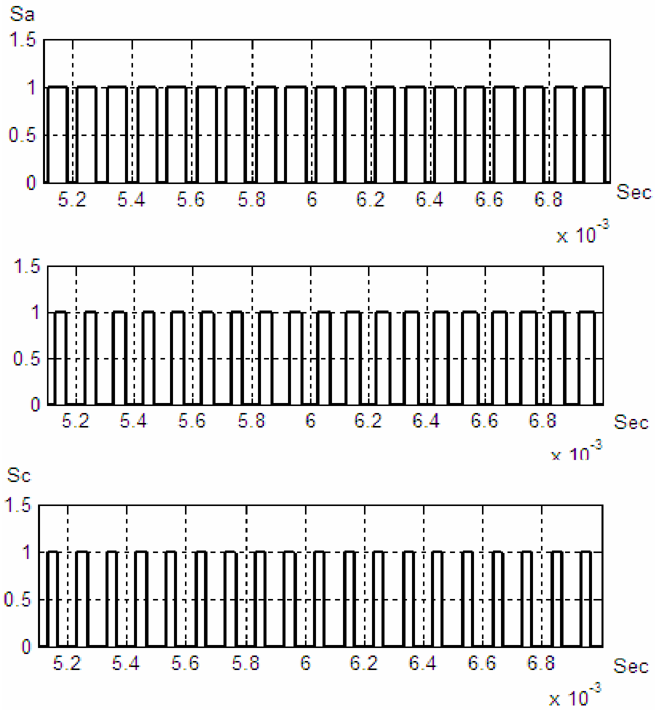

Fig. 3.27 Control signals for three upper switches of the inverter

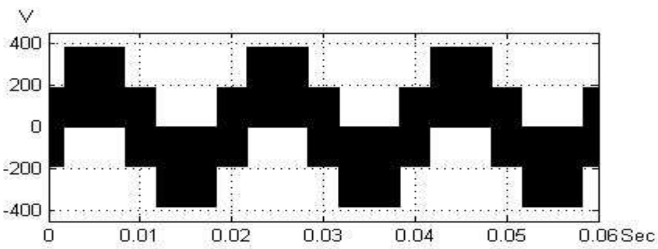

Fig. 3.28 Phase voltage of the motor Va

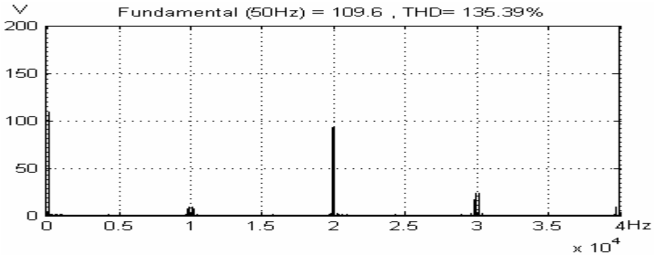

Fig. 3.29 Spectrum of phase voltage Va (peak value), and THD

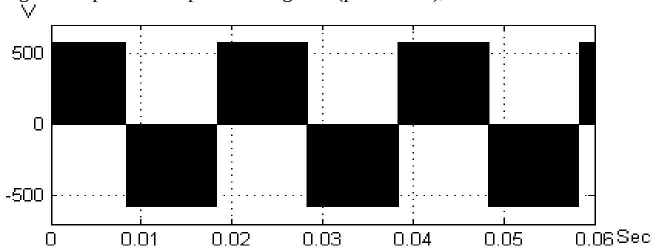

Fig. 3.30 Line voltage of the motor Vab

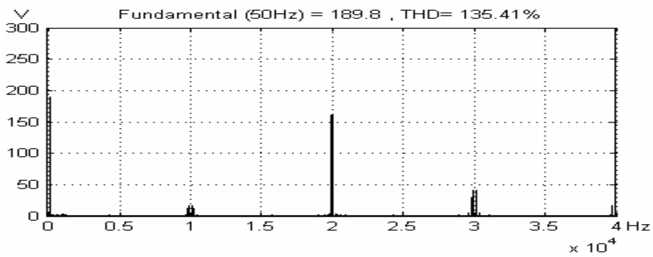

Fig. 3.31 Spectrum of Line voltage Vab (peak value), and THD

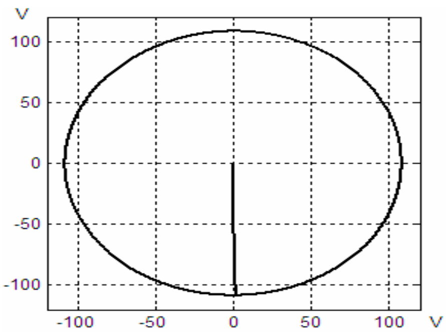

Fig. 3.32 Reference input voltage vector ($\alpha-\beta$)

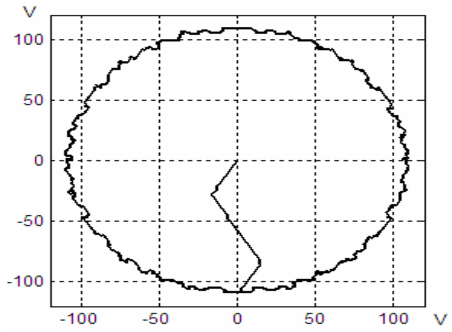

Fig. 3.33 Actual output voltage vector ($\alpha - \beta$)

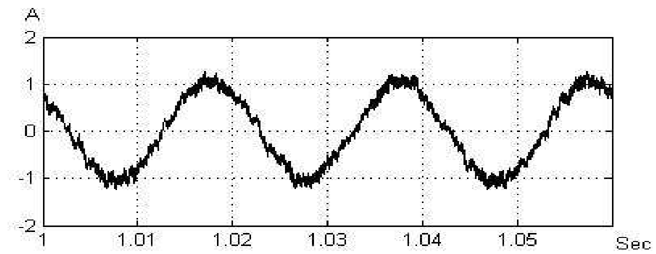

Fig. 3.34 Motor line current (Peak value) at half load Tl = 1.5 N.m

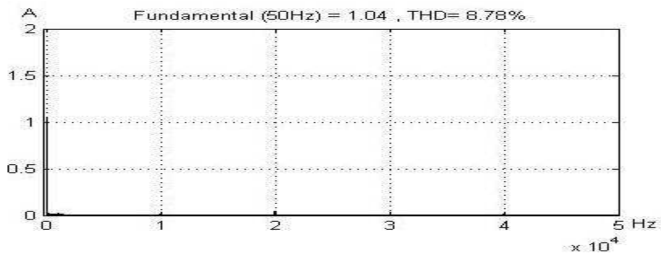

Fig. 3.35 Spectrum of motor line current (Peak value), and THD at half load Tl = 1.5 N.m

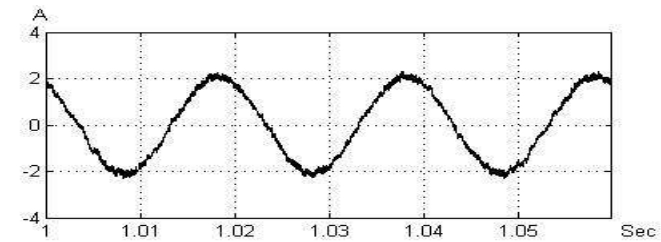

Fig. 3.36 Motor line current (Peak value) at full load Tl = 3 N.m

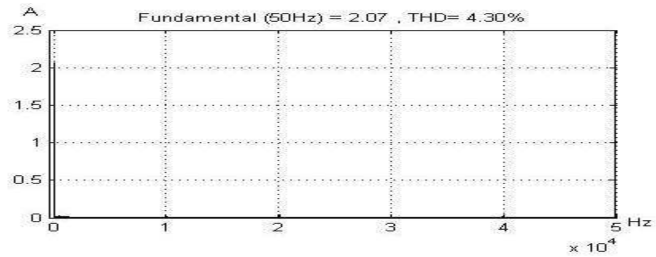

Fig. 3.37 Spectrum of motor line current (Peak value), and THD at full load Tl = 3 N.m

2-a 5 KHz switching frequency, 150Hz fundamental frequency, Vdc=570V, rated voltage= 230Vrms (325V peak), modulation index m=1.1404

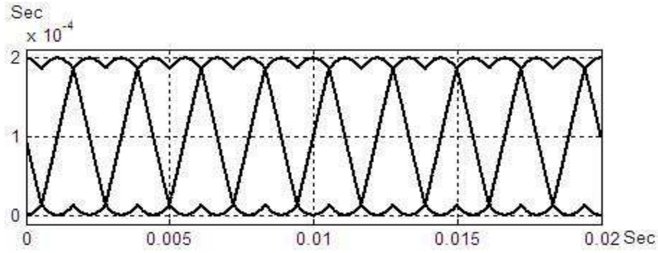

Fig. 3.38 Space vector modulating function a, b, c

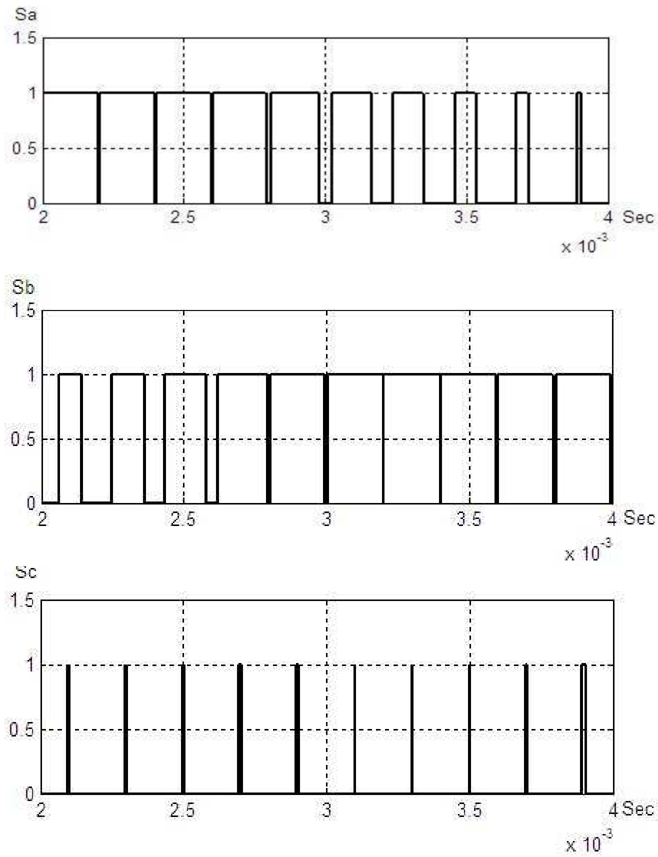

Fig. 3.39 Control signals for three upper switches of the inverter

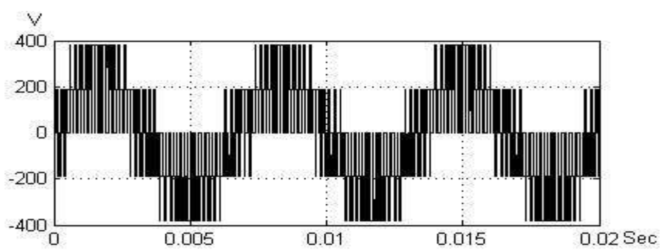

Fig. 3.40 Phase voltage of the motor Va

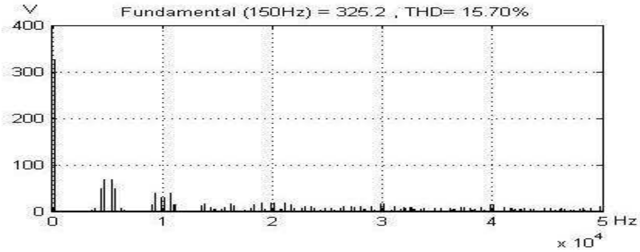

Fig. 3.41 Spectrum of phase voltage Va (peak value), and THD

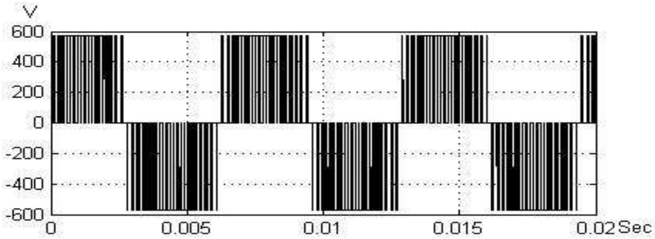

Fig. 3.42 Line voltage of the motor Vab

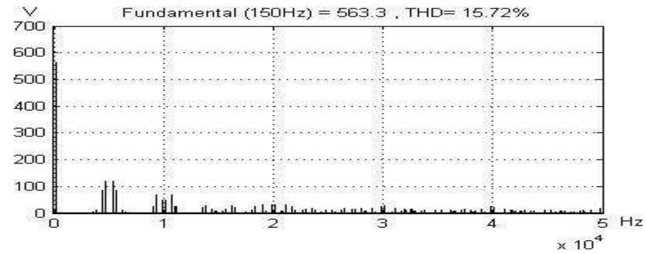

Fig. 3.43 Spectrum of Line voltage Vab (peak value), and THD

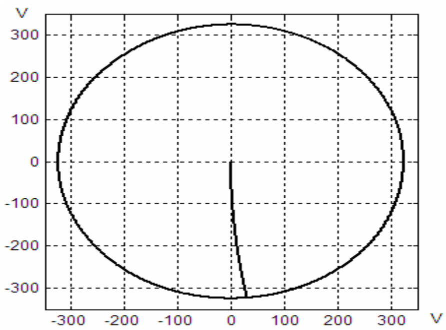

Fig. 3.44 Reference input voltage vector ($\alpha - \beta$)

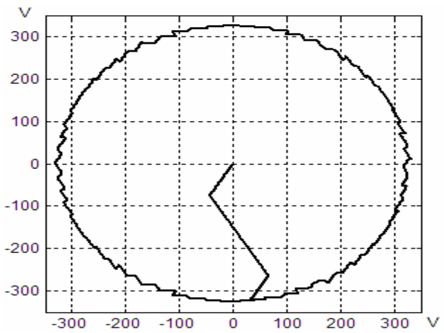

Fig. 3.45 Actual output voltage vector ($\alpha - \beta$)

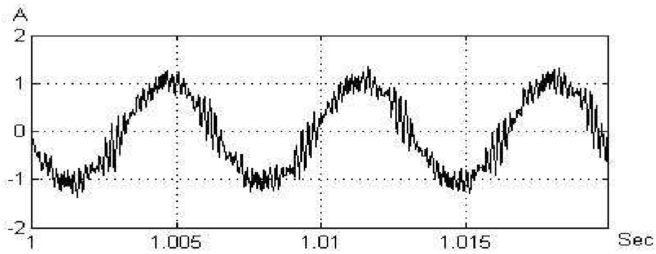

Fig. 3.46 Motor line current (Peak value) at half load Tl = 1.5 N.m

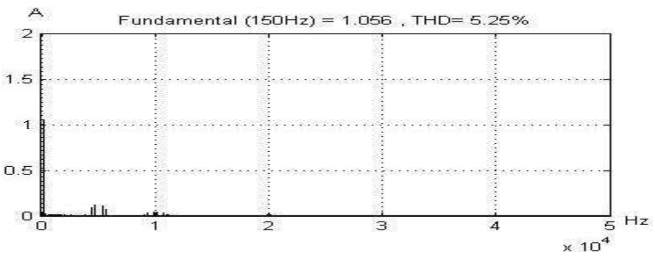

Fig. 3.47 Spectrum of motor line current (Peak value), THD at half load Tl = 1.5 N.m

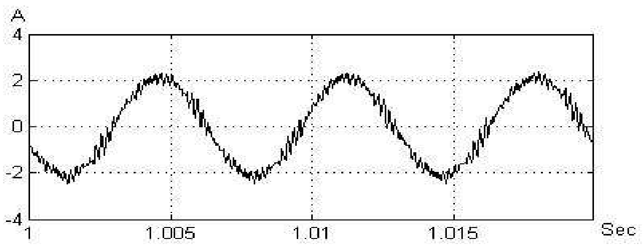

Fig. 3.48 Motor line current (Peak value) at full load Tl = 3 N.m

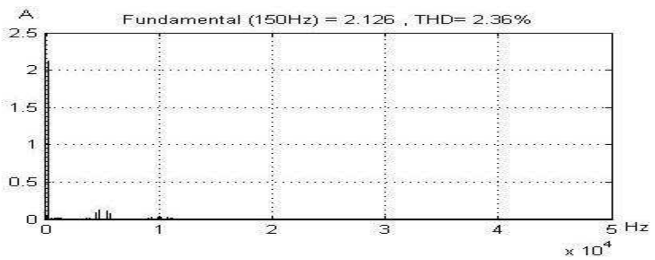

Fig. 3.49 Spectrum of motor line current (Peak value), THD at full load Tl = 3 N.m

2-b 5 KHz switching frequency, 50Hz fundamental frequency, Vdc=570V, rated voltage= 76.667 Vrms (108V peak), and modulation index m=0.38

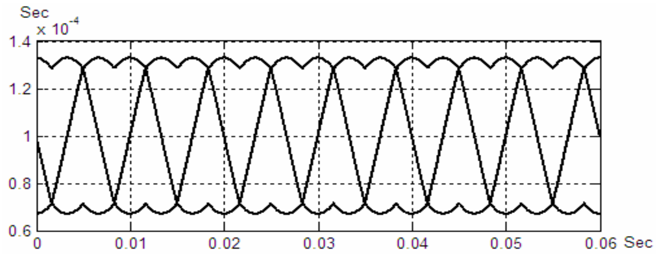

Fig. 3.50 Space vector modulating function a, b, c

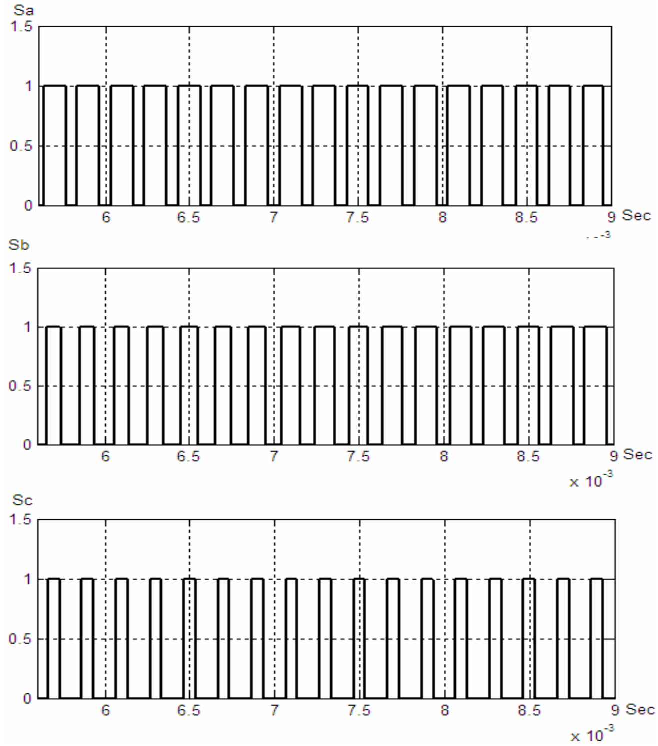

Fig. 3.50 Control signals for three upper switches of the inverter

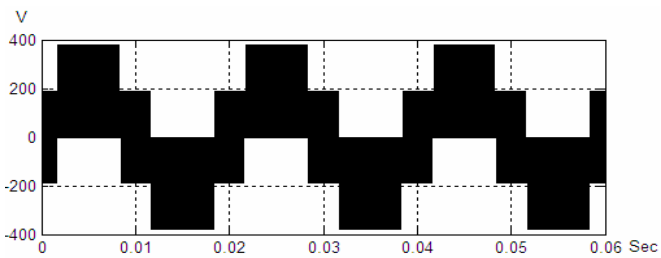

Fig. 3.51 Phase voltage of the motor Va

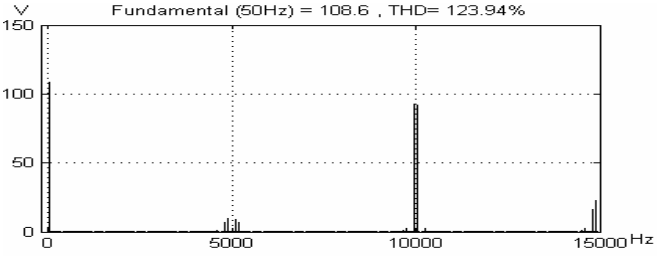

Fig. 3.52 Spectrum of phase voltage Va (peak value), and THD

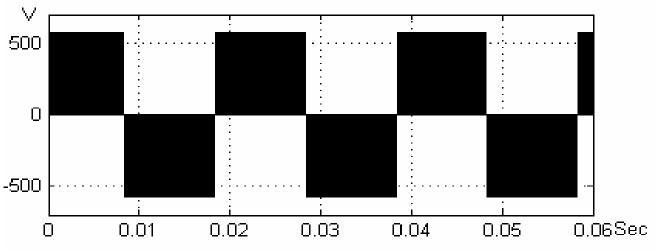

Fig. 3.53 Line voltage of the motor Vab

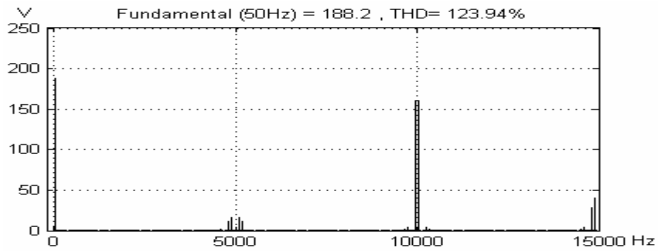

Fig. 3.54 Spectrum of Line voltage Vab (peak value), and THD

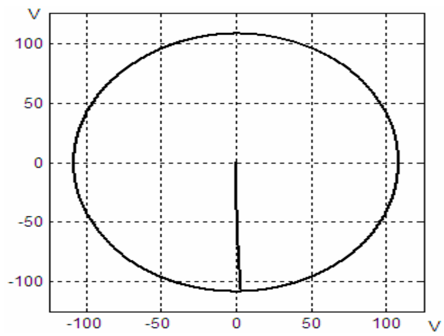

Fig. 3.55 Reference input voltage vector ($\alpha - \beta$)

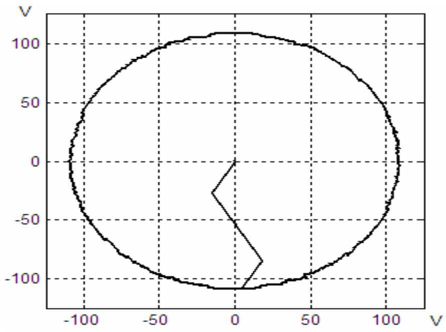

Fig. 3.56 Actual output voltage vector ($\alpha - \beta$)

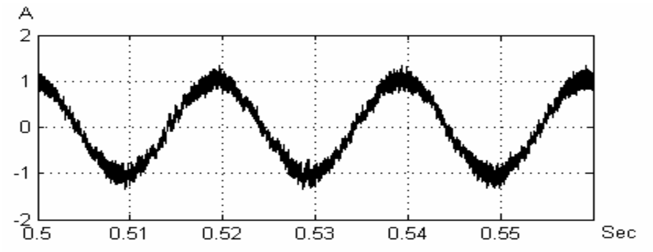

Fig. 3.57 Motor line current (Peak value) at half load Tl = 1.5 N.m

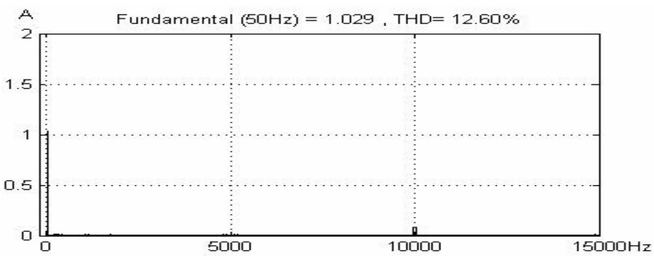

Fig. 3.58 Spectrum of motor line current (Peak value), THD at half load Tl = 1.5 N.m

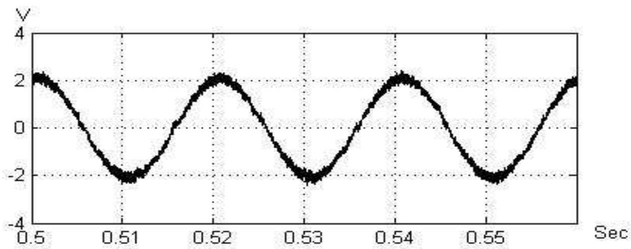

Fig. 3.59 Motor line current (Peak value) at full load Tl = 3 N.m

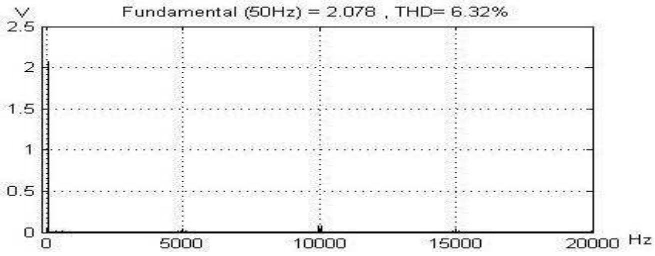

Fig. 3.60 Spectrum of motor line current (Peak value), THD at full load Tl = 3 N.m

Table 2 summaries the relation ship between the switching frequency, fundamental desired voltage frequency, phase voltage THD%, line voltage THD%, motor line current THD% at half load, and motor line current THD% at full load.

Switching frequency	Fundamental desired frequency	Output phase voltage THD%	Output line voltage THD%	Motor line current THD% at half load	Motor line current THD% at full load
10 KHz	150 Hz	10.45%	10.45%	7.20%	4.16%
	50 Hz	135.39%	135.41%	8.78%	4.30%
5 KHz	150 Hz	15.70%	15.725%	5.25%	2.36%
	50Hz	123.94%	123.94%	12.60%	6.32%

References:

[1] R. Arulmozhiyal, and K. Baskaran, "Space vector pulse width modulation based speed control of induction motor using fuzzy PI controller," *International Journal of Computer and Electrical Engineering*, vol. 1, no. 1, April 2009, pp. 98-103.
[2] A. Maamoun, A. Soliman, and A. M. Kheirelden, "Space-vector PWM inverter feeding a small induction motor," in *Proc. IEEE Int. Conf. on Mechatronics*, Komamoto, Japan, May 2007, pp. 1-4.
[3] W. Kaewjinda, and M. Konghirun, "Vector control drive of permanent magnet synchronous motor using resolver sensor," *ECTI Trans.Electrical Eng., Electronics, and Communications*, Thailand, vol. 5, no. 1, Feb. 2007, pp. 134-138.
[4] W.Zhang, and Y. Yu,"Comparison of three SVPWM strategies,"*Journal of Electronic Science and Technology of China*, vol. 5, no.3, Sept. 2007, pp. 283-387.
[5] A. Saadoun, A. Yousfi, and Y. Amirat, "Modeling and simulation of DSP controlled SVPWM three - phase VSI," *Journal of Applied Sciences*, vol. 7, no. 7, 2007, pp. 989-994.